Electrical Power and Energy Systems 44 (2013) 445–453

Contents lists available at SciVerse ScienceDirect

Electrical Power and Energy Systems

journal homepage: www.elsevier.com/locate/ijepes

Improving power quality of wind energy conversion system with unconventional power electronic interface

Lata Gidwani [a,*], Harpal Tiwari [b], R.C. Bansal [c]

[a] Department of Electrical Engineering, Government Engineering College, Ajmer, Rajasthan, India
[b] Department of Electrical Engineering, Malaviya National Institute of Technology, Jaipur, Rajasthan, India
[c] School of Information Technology & Electrical Engineering, The University of Queensland, St. Lucia, Australia

ARTICLE INFO

Article history:
Received 10 January 2012
Received in revised form 19 July 2012
Accepted 25 July 2012
Available online 26 September 2012

Keywords:
Doubly fed induction generator
Unconventional power electronic interface
Power quality
Total harmonic distortion
Wind energy conversion system

ABSTRACT

The increasing interest to utilize wind energy as a power source prompted more researches to be dedicated to the unconventional integration of this power source into the current grid. In this paper, one avenue to achieve this efficient utilization, through the use of integrated wind energy conversion system (WECS) using doubly fed induction generator (DFIG) is presented. Wind grid integration brings the problems of voltage fluctuation and harmonic distortion. This paper presents an Unconventional Power Electronic Interface (UPEI) to reduce the total harmonic distortion (THD) and enhance power quality during disturbances. The models used in the paper includes a pitch-angled controlled wind turbine model, a DFIG model, power system model and an UPEI having controlled converters. A phase to phase fault is simulated on 132 kV bus and the measured results obtained from grid connection of the wind generation system are presented. The results have demonstrated the ability of UPEI to regulate pitch angle, VAR and to reduce THD. The proposed system increases the effectiveness of the utilization of wind energy.

1. Introduction

The increasing demand of energy from the growing modern society has created a concern in the last few decades. This is made worse by the fact that most of the current energy sources are exhaustible and depleting rapidly. Moreover, the combustion process of most of the current energy sources such as coal and fuel produces a high level or air pollution that causes global warming, which is a currently emerging problem. These issues have prompted the rapid development of many renewable energy sources over recent years, particularly the clean and pollution free wind energy that has an eligible rate of depletion. Thus, many efforts are dedicated to efficiently integrate wind energy into the grid network [1,2]. However, electric utility grid systems cannot readily accept connection of new generation plant without power electronic interface. Recent developments have made the trade-off benefits exceed the cost premium of machine in the power ranges up to several 100 kW. Considering these trends, one of the best topologies for wind power conversion system is the full size AC–DC–AC converter [3,4].

Power quality has also been a growing concern in recent years with many researches done in this area [5,6]. Harmonic emissions are recognized as a power quality problem for modern variable-speed wind turbines (WTs). For this reason, relevant standards require the measurement of harmonics [7–10] and their inclusion in the power quality certificates of WTs, and grid interconnection assessment procedures always comprise provisions for their control [11,12]. In this paper, the WECS with UPEI capable of reducing THD noticeably during disturbances [13] is proposed. It has a pitch-angled controlled wind turbine model, a DFIG model, a power system model and UPEI having controlled converters. Simulations have been conducted with Matlab/Simulink software to validate the model and the control schemes. This wind energy conversion system has many advantages, such as low total harmonic distortion, long distance between generator and converter possible, able to stand wide transients of grid voltage and current, regulation of generator speed to 1 p.u., regulation of reactive power to zero MVAR, regulation of pitch angle to zero degree and thus increase power quality. This paper is organized as follows. Section 2 presents modeling of wind turbine with DFIG. Power electronic interface model is present in Section 3. Results and discussion are presented in Section 4. Finally important conclusions are summarized in Section 5.

2. Modeling of wind turbine with DFIG

Half of the world's leading wind turbine manufacturers use the DFIG systems. This is due to the fact that the power electronic

* Corresponding author. Address: 99 Balaji Nagar, Makarwali Road, Ajmer, Rajasthan, India.
E-mail addresses: lata_gidwani@rediffmail.com (L. Gidwani), harpaltiwari@yahoo.co.in (H. Tiwari), bansal@itee.uq.edu.au (R.C. Bansal).

0142-0615/$ - see front matter © 2012 Elsevier Ltd. All rights reserved.
http://dx.doi.org/10.1016/j.ijepes.2012.07.051

converter only has to handle a fraction (20–30%) of the total power, i.e., the slip power. This means that if the speed is in the range ±30% around the synchronous speed, the converter has a rating of 30% of the rated turbine power, reducing the losses in the power electronic converter, compared to a system where the converter has to handle the total power. In addition, the cost of the converter becomes lower. The WECS considered for analysis consist of a DFIG driven by a wind turbine, rotor side converter, DC to DC intermediate circuit and grid side converter. Fig. 1 shows a schematic diagram of WECS having DFIG and UPEI that will be discussed in this paper. The mechanical power available from a wind turbine

$$P_w = 0.5\rho\pi R^2 V_w^3 C_p(\lambda,\beta) \tag{1}$$

where P_w is the extracted power from the wind, ρ is the air density, R is the blade radius, and V_w is the wind speed. C_p is called the 'power coefficient', and is given as a nonlinear function of the parameters tip speed ratio λ and blade pitch angle β. Here the following function will be used [14]

$$C_p = \frac{1}{2} * (\lambda - 0.022 * \beta^2 - 5.6) * e^{-0.17\lambda} \tag{2}$$

$$\lambda = \frac{V_w}{\omega_B} \tag{3}$$

where ω_B is the rotational speed of turbine. Usually C_p is approximated as [15]

$$C_p = \alpha\lambda + \beta\lambda^2 + \gamma\lambda^3 \tag{4}$$

where α, β and γ are constructive parameters for a given turbine. The torque developed by the windmill is

$$T_t = 0.5\rho\left(\frac{C_p}{\lambda}\right)V_w^3\pi R^2 \tag{5}$$

The equation of rotor motion is given as

$$\frac{d\omega_r}{dt} = \frac{2P_a}{J\omega_r} \tag{6}$$

where J is the moment of inertia due to the rotating mass and P_a is the rotor acceleration mechanical power. The angular velocity of the rotor is considered in the region $0.7\omega \leqslant \omega_r \leqslant 1.3\omega$ for the case study presented in this paper. The DFIG equations can be written as [16]

$$\frac{d\lambda_{ds}}{dt} = u_{ds} - R_s i_{ds} + \omega_r \lambda_{qs} \tag{7}$$

$$\frac{d\lambda_{qs}}{dt} = u_{qs} - R_s i_{qs} - \omega_r \lambda_{ds} \tag{8}$$

$$\frac{d\lambda_{dr}}{dt} = u_{dr} - R_r i_{dr} + s\omega_r \lambda_{qr} \tag{9}$$

$$\frac{d\lambda_{qr}}{dt} = u_{qr} - R_r i_{qr} - s\omega_r \lambda_{dr} \tag{10}$$

The stator electric values are indicated by the subscript s and the rotor electric values are indicated by the subscript r. u is a voltage, R is a resistance, i is a current, λ is a flux linkage. ω is the stator electrical frequency and s is rotor slip. The flux linkages are given by [16]

$$\lambda_{ds} = L_s i_{ds} + L_m i_{dr} \tag{11}$$

$$\lambda_{qs} = L_s i_{qs} + L_m i_{qr} \tag{12}$$

$$\lambda_{dr} = L_r i_{dr} + L_m i_{ds} \tag{13}$$

$$\lambda_{qr} = L - s i_{qr} + L_m i_{qs} \tag{14}$$

L_s, L_r are the stator and the rotor leakage inductance respectively and L_m is the mutual inductance between the stator and the rotor.

Fig. 2 shows turbine power characteristics for zero degree pitch angle. The power is controlled in order to follow a pre-defined power–speed characteristic, named tracking characteristic. This characteristic is illustrated in the Fig. 2 by the dotted ABCD curve superimposed to the mechanical power characteristics of the turbine obtained at different wind speeds. The dashed line in Fig. 2 indicates maximum power at base wind speed (11 m/s) and pitch angle zero degree.

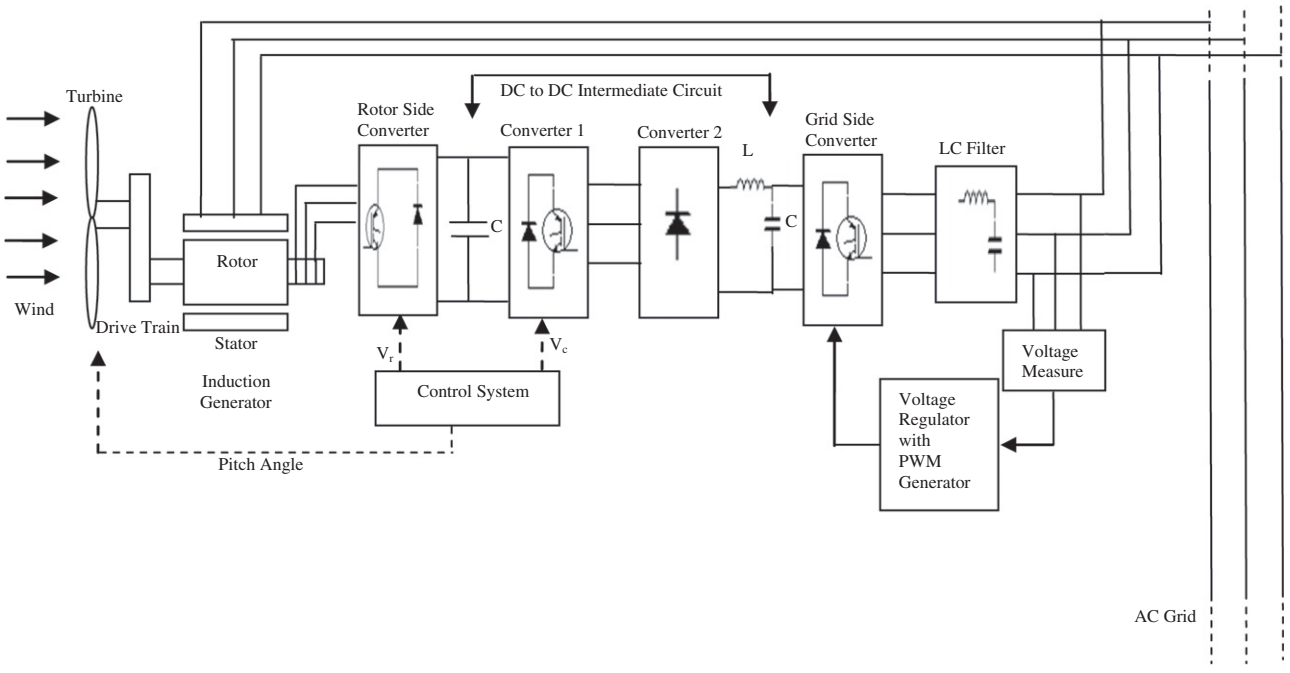

Fig. 1. Proposed wind energy conversion system with DFIG and controlled UPEI.

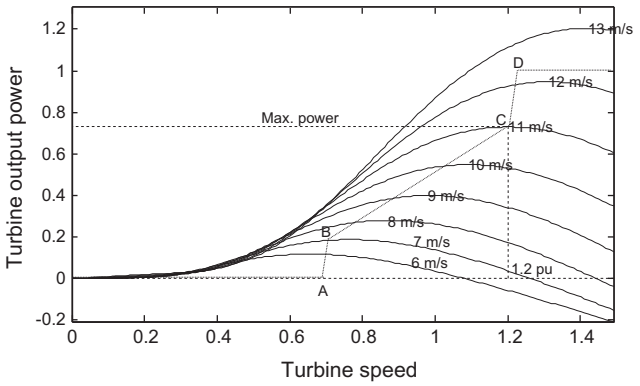

Fig. 2. Turbine power characteristics.

3. Unconventional power electronic interface model

3.1. Rotor side converter

Rotor side converter consists of three-phase IGBT-diode rectifier connected in Graetz bridge configuration with snubber resistance and capacitance. The values of snubber resistance R_s and snubber capacitance C_s for rotor converter are derived from the following criteria:

- The snubber leakage current at fundamental frequency is less than 0.1% of nominal current when power electronic devices are not conducting.
- The time constant (RC) of snubbers is higher than two time sample time ($2 \times T_s$).

The circuit is discretized at a sample time of 2 μsec. Fig. 3 shows voltage and VAR regulation of rotor side converter. A

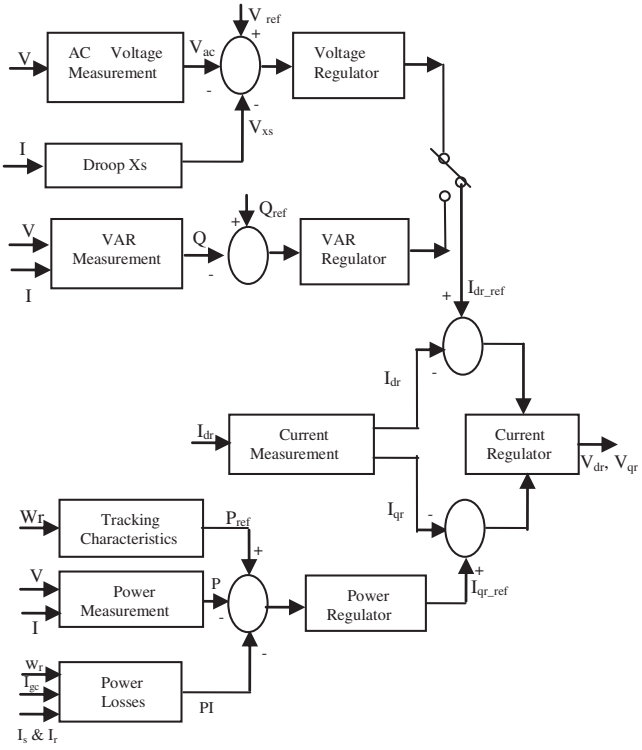

Fig. 3. Voltage and VAR regulator of rotor side converter.

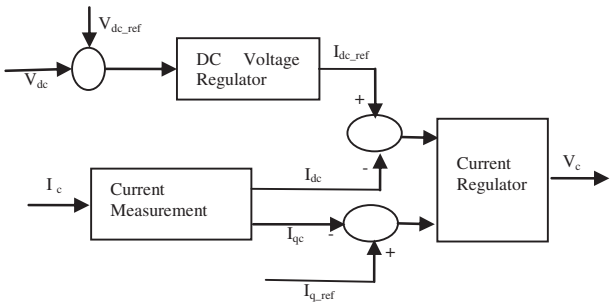

Fig. 4. Voltage and current regulators of converter 1.

Proportional–Integral (PI) regulator is used to reduce the power error to zero. The actual component of positive-sequence current (I_{qr}) is compared to I_{qr_ref} and the error is reduced to zero by a current regulator (PI). The output voltage of this regulator is q-axis rotor voltage V_{qr}. The reactive power at grid terminals is kept constant by a VAR regulator.

The output of the voltage regulator or VAR regulator is d-axis reference rotor current I_{dr_ref} which is injected in the rotor by rotor converter. The same current regulator is used to regulate the actual component of positive-sequence current (I_{dr}). The output of this regulator is the d-axis rotor voltage V_{dr}.

3.2. DC to DC intermediate circuit

As shown in Fig. 1, DC to DC intermediate circuit consists of two converters: converter 1 (DC to AC) and Converter 2 (AC to DC). The control system of converter 1, illustrated in the Fig. 4 consists of:

- Measurement systems which measure d-axis and q-axis components of AC positive-sequence currents to be controlled as well as the DC voltage V_{dc}.
- An outer regulation loop which consists of a DC voltage regulator. The output of the DC voltage regulator is the reference DC current I_{dc_ref} for the current regulator (I_{dc} = current in phase with grid voltage which controls active power flow).
- An inner current regulation loop which consists of a current regulator. The current regulator controls the magnitude and phase of the voltage generated by converter (V_c) from the I_{dc_ref} produced by the DC voltage regulator and specified I_{q_ref}.

The pitch angle is regulated at zero degree by pitch angle regulator until the speed w_r reaches desired speed of the tracking characteristic w_d. Beyond w_d, the pitch angle is proportional to the speed deviation from desired speed. The control system is illustrated in Fig. 5. The AC output voltage obtained at converter 1 is rectified by converter 2, which is a six pulse diode bridge.

3.3. Grid side converter system

The DC voltage output from intermediate circuit is applied to grid side converter, which consists of an IGBT two-level inverter,

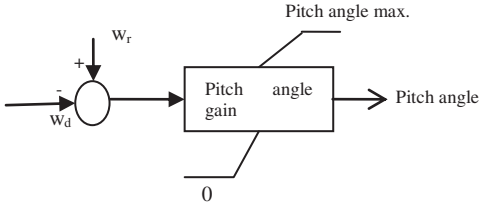

Fig. 5. Pitch control system.

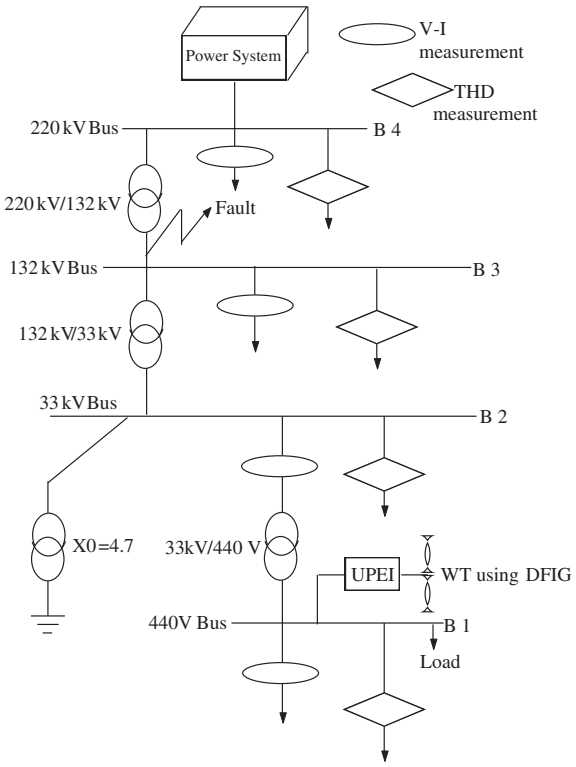

Fig. 6. Power system model used in paper.

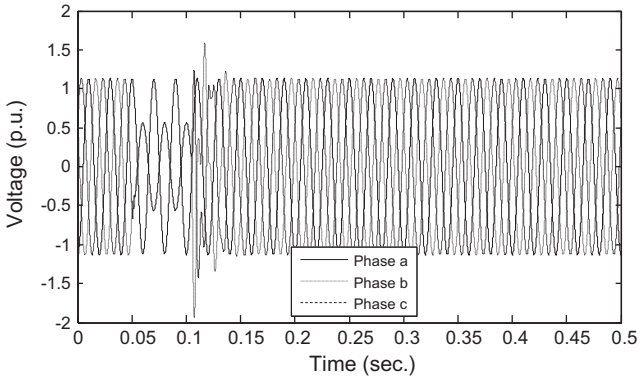

Fig. 7. Case I: 3-phase voltage waveform at bus B1.

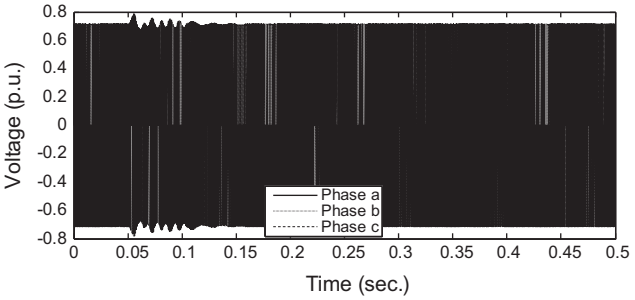

Fig. 8. 3-Phase voltage waveform at output of DFIG.

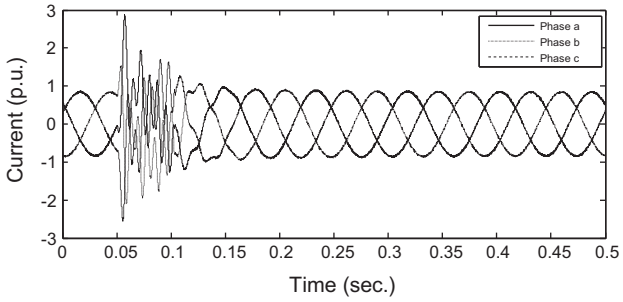

Fig. 9. 3-Phase current waveform at output of DFIG.

generating AC voltage at 50 Hz. The IGBT inverter uses Pulse Width Modulation (PWM) at 2000 Hz carrier frequency. The load voltage is regulated at 440 V rms by a PI voltage regulator using abc to dq and dq to abc transformations. The output of voltage regulator is a vector containing three modulating signals used by the PWM Generator to generate the 6 IGBT pulses. The another output gives the modulation index m.

4. AC power grid model

The WECS having UPEI is connected to a 33 kV distribution system exports power to a 220 kV grid as shown in Fig. 6. A and B fault at $t = 0.104$ s for a duration of 3 ms is simulated at B3. The wind speed is maintained constant at 10 m/s. The control system shown in Section 3 is used to maintain the speed at 1 p.u. and to regulate reactive power produced by the wind turbine at zero MVAR.

5. Results and discussion

In this section the results obtained through simulations for the grid connection of the DFIG using the power electronic interface and control system described above are presented. Three different cases are considered now. Simulations of power system model are run without DFIG wind turbines i.e. the wind turbines are not connected to the transmission system during Case-I. A phase to phase fault is simulated on 132 kV line at $t = 0.05$ s for 50 ms. The voltage waveforms at bus B1 is shown in Fig. 7. As clear from this figure, the voltage at bus B1 oscillates due to fault at $t = 0.05$ s, but oscillations die out quickly and returns to normal values after approx. 0.1 s. Simulations are carried out in Matlab/Simulink with 9 MW wind-farm using DFIG connected to power system along with conventional back to back converter during Case-II. The fault conditions are kept same as before. The output voltage and current waveforms of DFIG are shown in Figs. 8 and 9. The voltage and current oscillates during fault but returns to steady-state value in reasonable time of 0.15 s. The voltage waveforms at bus B1 during Case-II is shown in Fig. 10. The voltage waveforms at bus B1 oscillate more during present case (Case-II) as compared to Case-I. Also voltage oscillations die out in comparatively more time than Case-I. As seen in Fig. 10, the voltage at bus B1 returns to its steady-state value at about $t = 0.37$ s in Case-II, while it reaches steady-state value at about $t = 0.15$ s (Fig. 7) in Case-I. Hence the integration of DFIG wind turbine in power system introduces greater voltage fluctuations in it and power quality is deteriorated. The power quality needs to be enhanced and for that purpose, Unconventional Power Electronic Interface (UPEI) is proposed.

In Case-III, DFIG is connected to power grid through unconventional power electronic interface proposed in this paper. Simulations are conducted using Matlab/Simulink and results are presented here. Active power at wind turbine against time is shown in Fig. 11. The active power oscillates due to fault at $t = 0.05$ s and it comes to its steady-state value in reasonable time

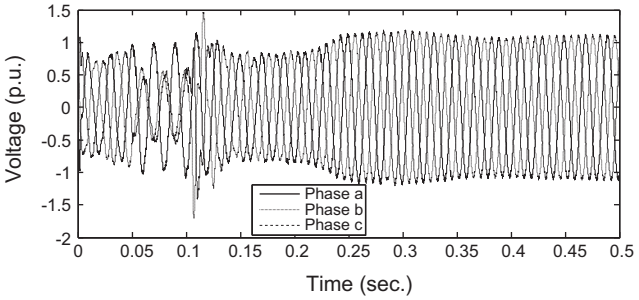

Fig. 10. Case II: 3-phase voltage waveform at bus B1.

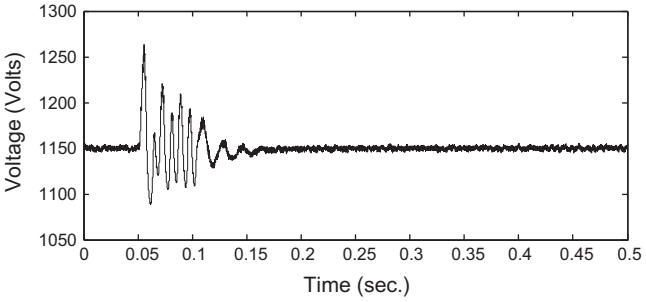

Fig. 14. DC output voltage waveform of DC to DC intermediate circuit.

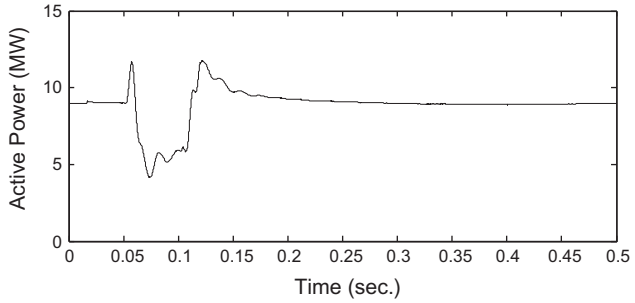

Fig. 11. Active power output of DFIG.

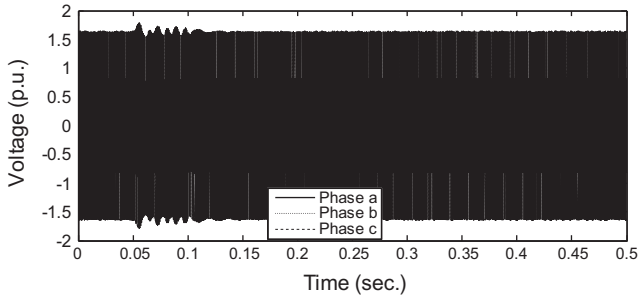

Fig. 15. 3-Phase voltage waveform of grid side converter.

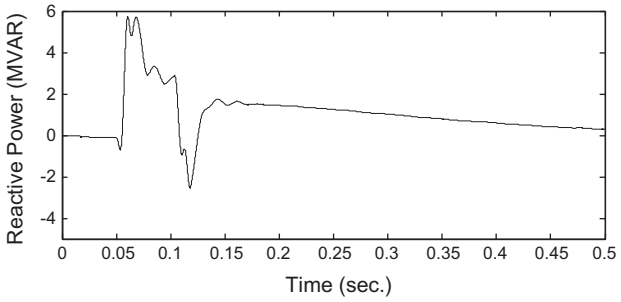

Fig. 12. Reactive power output of DFIG.

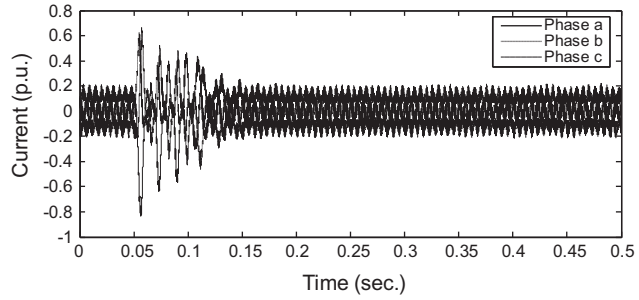

Fig. 16. 3-Phase current waveform of grid side converter.

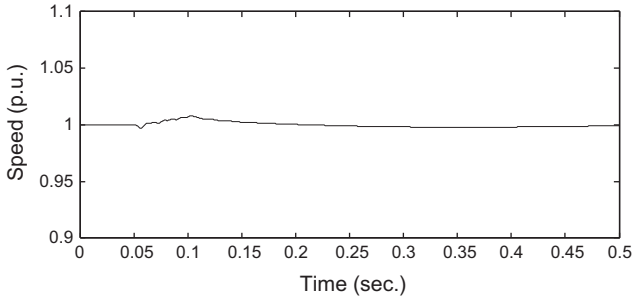

Fig. 13. Generator rotor speed.

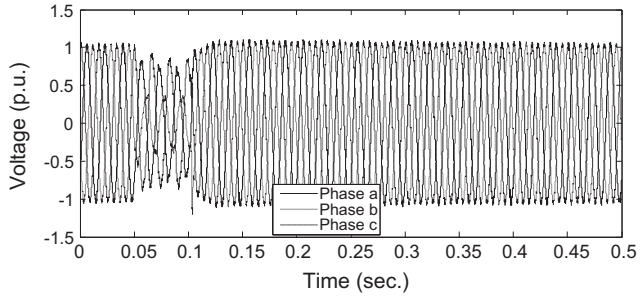

Fig. 17. Case III: 3-Phase voltage waveform at bus B1.

of 0.15 s. The variation of reactive power of DFIG is shown in Fig. 12. During fault, the control system tries to regulate the reactive power to zero MVAR. The system recovers after sometime and the reactive power of DFIG returns to zero MVAR after oscillations due to clearing of fault. Fig. 13 shows generator rotor speed. The deviation in rotor speed from 1 p.u. is much less and hence the control system is effective in maintaining rotor speed constant at 1 p.u. The dc output voltage of DC to DC intermediate circuit is shown in Fig. 14. The DC voltage is regulated at 1150 V.

During the fault, the control system tries to regulate DC voltage at 1150 V. The system recovers and the control system is effective in regulating DC voltage at 1150 V. Fig. 15 shows phase voltages

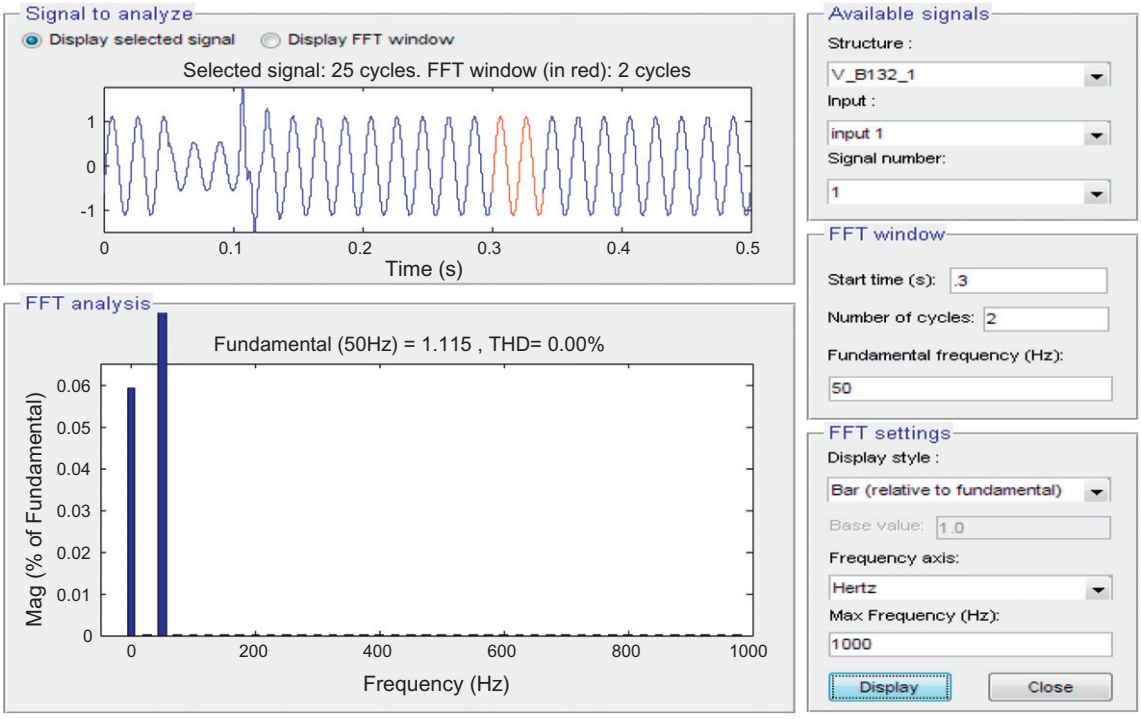

Fig. 18. FFT analysis of voltage at bus B3 during Case-I.

V_{a0}, V_{b0} and V_{c0} flowing into grid side converter, while phase currents I_{a0}, I_{b0}, I_{c0} flowing into the grid side converter are shown in Fig. 16. Phase voltage waveforms at bus B1 is presented in Fig. 17. As clear from Figs. 15–17, the phase voltages and currents at grid side converter and bus B1 oscillate due to phase to phase fault from $t = 0.05$ s to $t = 0.15$ s, but they return to their normal values in a reasonable time.

Now three cases are compared i.e. wind energy generation system without DFIG wind turbines, wind energy generation system with DFIG wind turbines along with conventional back to back converter connected to grid and wind generation system with DFIG wind turbines along with unconventional UPEI connected to grid are compared. The FFT tool of powergui is used to display the frequency spectrum of voltage and current waveforms. FFT analysis of

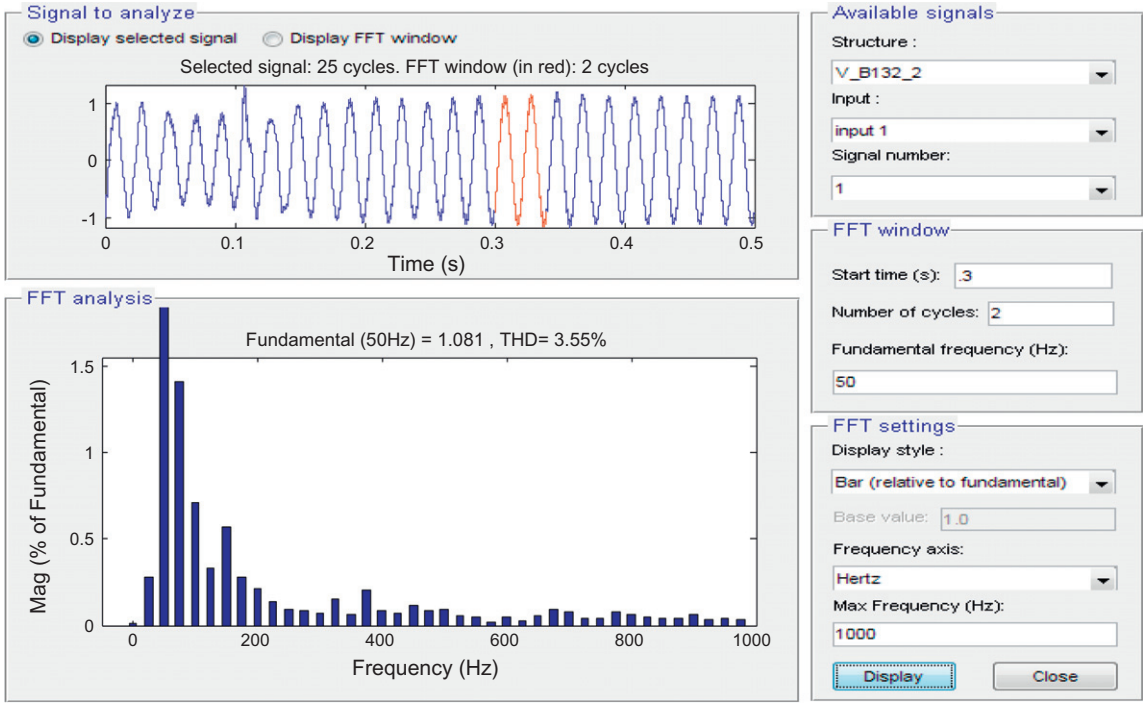

Fig. 19. FFT analysis of voltage at bus B3 during Case-II.

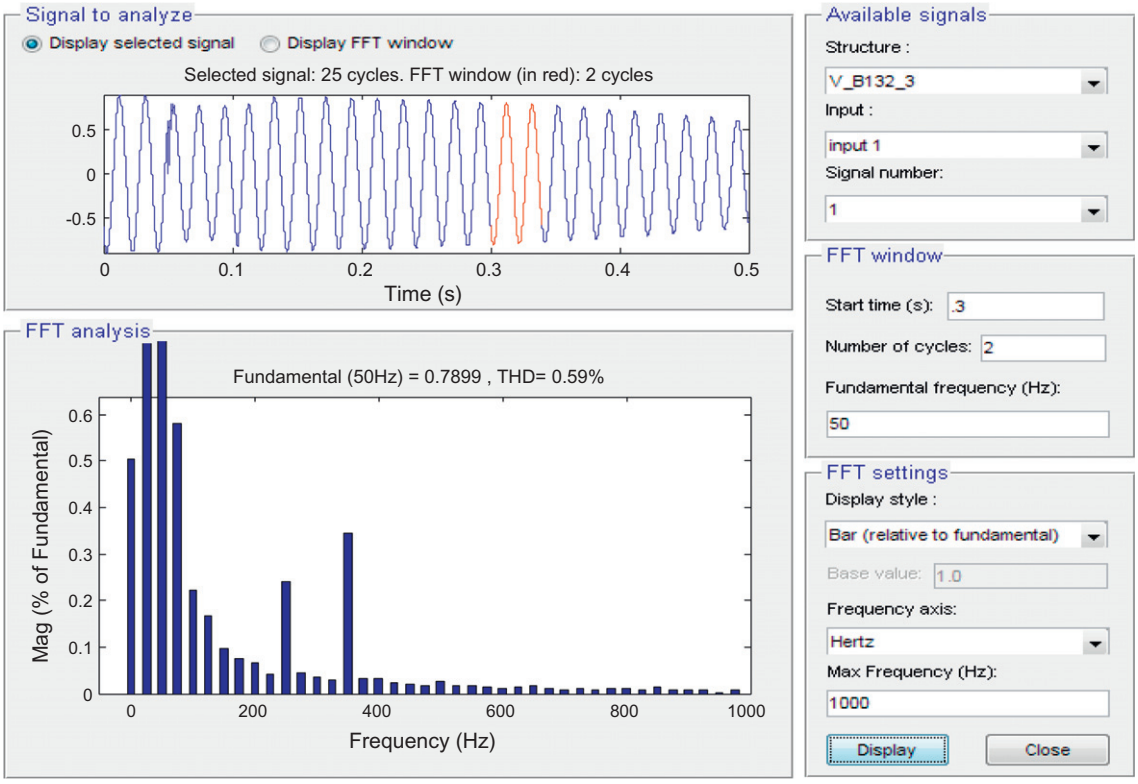

Fig. 20. FFT analysis of voltage at bus B3 during Case-III.

voltage at bus B3 during different cases is shown in Figs. 18–20 and FFT analysis of current at bus B3 during different cases is shown in Figs. 21–23. Harmonics are displayed in percent of the fundamental component. The voltage THD and current THD at various buses during different cases is presented in Tables 1 and 2 respectively.

It is observed that THD at buses B1, B2, B3 and B4 are more in Case-II as compared to Case-I. This is because connection of grid with wind turbine increases harmonics in voltage and current waveforms as wind energy depends on flow of wind which is random in nature. As clear from Tables 1 and 2, THD increases

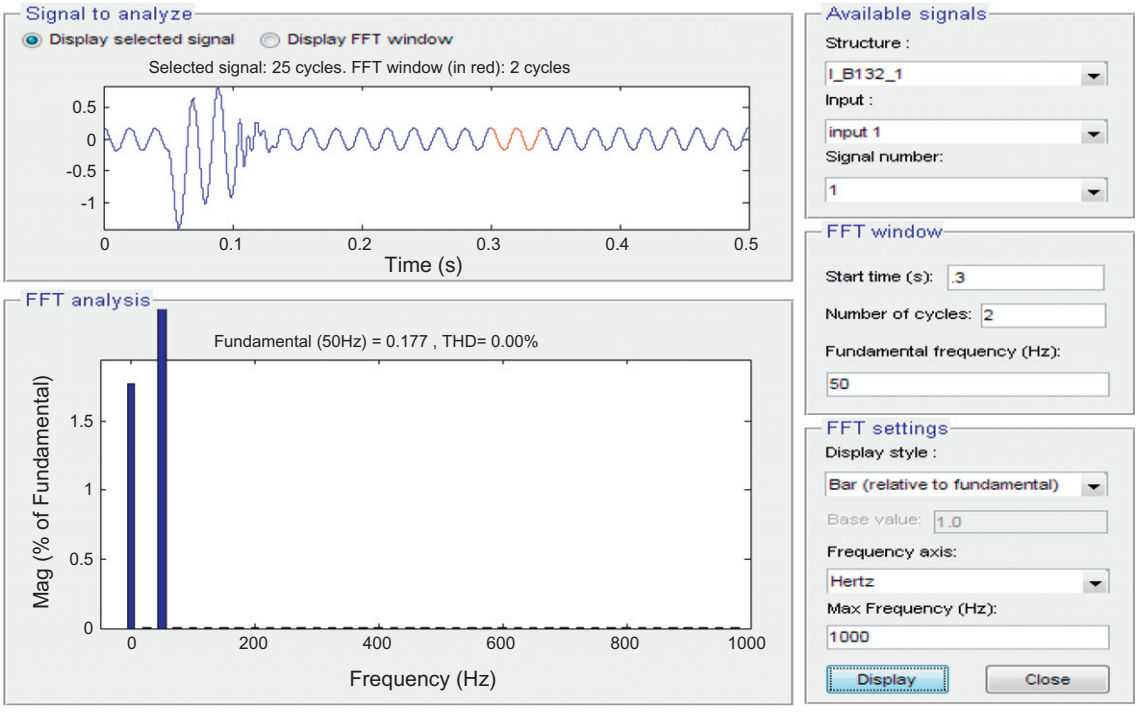

Fig. 21. FFT analysis of current at bus B3 during Case-I.

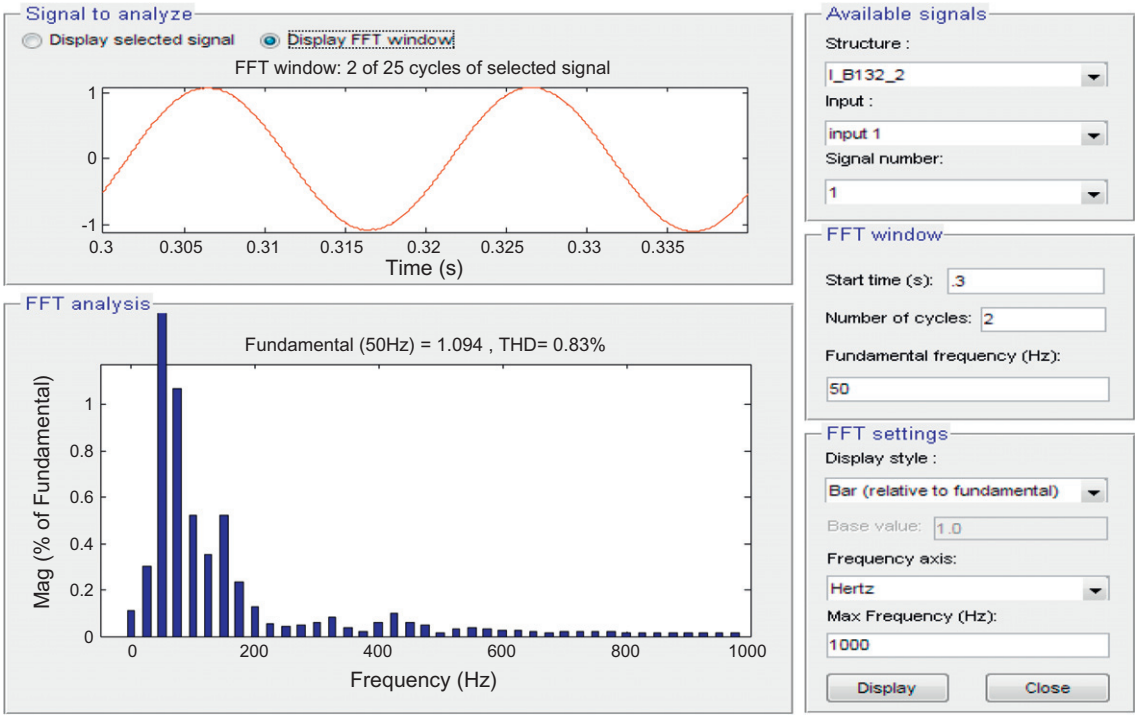

Fig. 22. FFT analysis of current at bus B3 during Case-II.

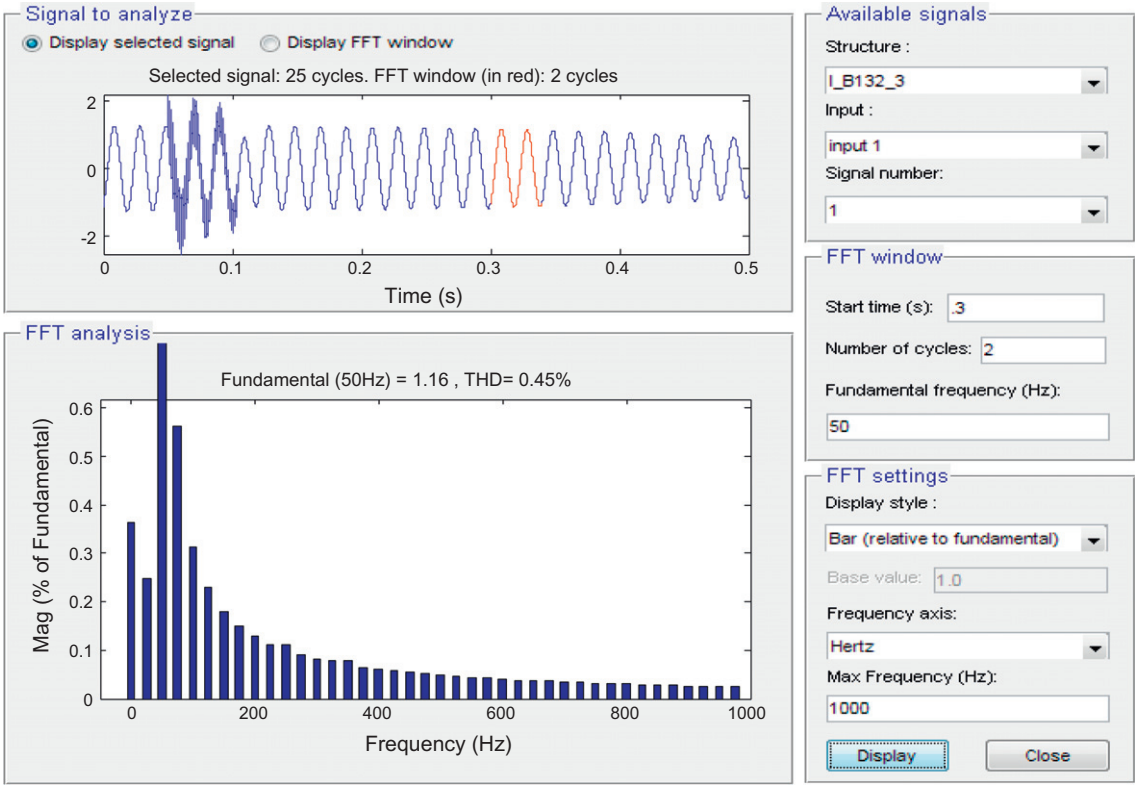

Fig. 23. FFT analysis of current at bus B3 during Case-III.

on integration of wind energy using DFIG into power grid in Case-II as compared to Case-I. On inclusion of UPEI in power grid integrated with DFIG wind turbines, THD decreases in Case-III as compared to Case-II. It shows the effectiveness of UPEI in DFIG wind integrated power systems. It is clear from the figures that THD values are much less for Case-III, particularly for buses B3 and B4, in which unconventional proposed interface is used as compared to Case-II, in which conventional back to back converters are used.

Table 1
Comparison of voltage THD.

Voltage THD at	Case-I (%)	Case-II (%)	Case-III (%)
Bus B1	0.00	3.56	3.43
Bus B2	0.00	3.55	2.45
Bus B3	0.00	3.55	0.59
Bus B4	0.00	3.26	0.36

Table 2
Comparison of current THD.

Current THD at	Case-I (%)	Case-II (%)	Case-III (%)
Bus B1	0.00	3.17	2.2
Bus B2	0.00	3.11	0.57
Bus B3	0.00	0.83	0.45
Bus B4	0.00	0.04	0.02

The results have clearly demonstrated the ability of proposed system to reduce the transients and harmonic distortion in power system and thus enhance the power quality.

6. Conclusions

This paper has presented the detailed model of the variable speed wind turbine with DFIG connected to AC grid through UPEI. At the same time, the paper addresses control schemes of the wind turbine in terms of pitch angle control, AC and DC voltage regulation, VAR regulation and current regulation of converter systems. Three different cases are considered and results obtained are compared to demonstrate the ability of power electronic interface having control system in event of transient fault. The results obtained indicate that the variations in voltages at different locations in power system model are much less in Case-III (with DFIG and UPEI) as compared to Case-II (with DFIG). They return to steady-state values after experiencing oscillations for much less time during Case-III (with DFIG and UPEI). The control system is effective in regulating generator speed at 1 p.u. and reactive power at zero MVAR. Also the voltage THD and current THD at various buses of power system reduces during Case-III (with DFIG and UPEI). As a whole, it can be concluded that the proposed wind energy conversion system can enhance the power quality of system during a transient fault and maintain the output reactive power at zero MVAR, rotor speed to 1 p.u., pitch angle to zero degree and also reduces THD at various locations in power system.

References

[1] Chen Z, Spooner E. Grid interface for renewable energy sources. In: 2nd International power electronics and motion control conference (IPEMC'97), Hangzhou, China, November 1997. p. 256–61.
[2] Tiwari HP, Gidwani L. Wind energy-present scenario. Electr India Mag 2010;50(4):68–77.
[3] Rodriguez J, Bernet S, Wu B, Pontt JO, Kouro S. Multilevel voltage-source-converter topologies for industrial medium-voltage drives. IEEE Trans Ind Electron 2007;54(6):2930–45.
[4] Franquelo LG, Rodriguez J, Leon JI, Kouro S, Portillo R, Prats MM. The age of multilevel converters arrives. IEEE Trans Ind Electron Mag 2008;2(2):28–39.
[5] Altas IH, Ozkop E, Sharaf AM. A novel active filter strategy for power mitigation and quality enhancements in a stand-alone WECS. In: International conference on electrical and electronics engineering, Bursa; 2009. p. 88–91.
[6] Nishikata S, Tatsuta F. A new interconnecting method for wind turbine/generators in a wind farm and basic performances of the integrated system. IEEE Trans Ind Electron 2010;57(2):468–75.
[7] Lian KL, Noda T. A time-domain harmonic power-flow algorithm for obtaining nonsinusoidal steady-state solutions. IEEE Trans Power Delivery 2010;25(99):1–11.
[8] Papathanassiou SA, Papadopoulos MP. Harmonic analysis in a power system with wind generation. IEEE Trans Power Delivery 2006;21(4):2006–16.
[9] Chang GW, Chen CI, Teng YF. Radial-basis-function-based neural network for harmonic detection. IEEE Trans Ind Electron 2010;57(6):2171–9.
[10] Chang G, Chen C. Virtual instrumentation and educational platform for time-varying harmonics and interharmonics detection. IEEE Trans Ind Electron 2010;57(10):3334–42.
[11] Papathanassiou SA. A technical evaluation framework for the connection of DG to the distribution network. Electr Power Syst Res 2007;77(1):24–34.
[12] Taghizadeh H, Hagh MT. Harmonic elimination of cascade multilevel inverters with non-equal DC sources using particle swarm optimization. IEEE Trans Ind Electron 2010;57(11):3678–84.
[13] Gidwani L, Tiwari HP, Kumar R. Wind energy integration in electrical power grid: simulation of transient fault behaviour and analysis. J Electr Eng 2009;9:77–85.
[14] Perdana A, Carlson O, Persson J. Dynamic response of grid connected wind turbine with doubly fed induction generator during disturbances. Nordic workshop on power and industrial electronics, Trondheim; 2004. p. 1–7.
[15] Mayosky MA, Cancelo GIE. Adaptive control of wind energy conversion systems using radial basis networks. In: Neural networks proceedings, IEEE world congress on computational intelligence, 4–9 May, vol. 2; 1998. p. 996–1001.
[16] Slootweg JG, Polinder H, Kling WL. Dynamic modelling of a wind turbine with doubly fed induction generator. Power engineering society summer meeting, Vancouver, BC, vol. 1; 2001. p. 644–9.